

Apparent Double SiO Maser Sources

Shuji DEGUCHI,¹ Takahiro FUJII,^{2,3} Hideyuki IZUMIURA,⁴ Shigeru MATSUMOTO,^{2,3}
Yoshikazu NAKADA,^{3,5} Peter R. WOOD,⁶ and Issei YAMAMURA^{2,3,7}

¹*Nobeyama Radio Observatory, National Astronomical Observatory,
Minamimaki, Minamisaku, Nagano 384-1305*

²*Department of Astronomy, The University of Tokyo, Bunkyo, Tokyo 113-0032*

³*Institute of Astronomy, The University of Tokyo, Mitaka, Tokyo 181-8588*

⁴*Okayama Astrophysical Observatory, National Astronomical Observatory,
Kamogata, Asakuchi, Okayama 719-0200*

⁵*Kiso Observatory, Institute of Astronomy, The University of Tokyo, Mitake, Kiso, Nagano 397-0101*

⁶*Mount Stromlo and Siding Spring Observatories,
Private Bag, Weston Creek PO, Canberra, ACT 2611, Australia*

⁷*Sterrenkundig Instituut "Anton Pannekoek", Universiteit van Amsterdam,
Kruislaan 403, 1098 SJ Amsterdam, The Netherlands*

(Received 1998 December 22; accepted 1999 April 5)

Abstract

During the course of a SiO maser survey of galactic disk IRAS sources at 43 GHz, we found two cases of doubly peaked SiO maser sources in the 40'' half-power beam of the Nobeyama 45-m telescope. The double peaks in the spectra of these sources (IRAS 18019–1822 and 18465–0717) have velocity separations of 73 and 147 km s⁻¹, indicating that each peak comes from a separate source. Infrared imaging observations found pairs of candidate counterparts for each source with angular separations of about 20''. Combining the observational data, we conclude that these objects are apparent-double SiO sources, which are by chance seen in the same direction. The discovery rate for pairs of SiO maser sources in a single telescope beam is found to be consistent with the surface density of SiO maser sources in the galactic disk. These sources can be used to measure the parallaxes and proper motions with VLBI in the future.

Key words: Infrared: sources — Masers — Stars: long-period variables

1. Introduction

OH/H₂O/SiO maser sources often exhibit double peaks in their spectra. They very often indicate emission from the front and rear parts of an outflow (Elitzur et al. 1976 for OH 1612 MHz emission), or emission from an expanding rotating disk (Wright et al. 1995 for SiO). The velocity separations of the OH 1612 MHz double peaks are typically 10–50 km s⁻¹ (for example, Reid, Moran 1981), suggesting an outflow with a velocity of about 5–25 km s⁻¹ (half of the velocity separation of the OH peaks) in the outer envelope of the Asymptotic Giant Branch (AGB) stars.

During the course of a SiO maser survey of IRAS sources in the galactic disk with the Nobeyama 45-m telescope (see Izumiura et al. 1999), we found two cases of doubly peaked SiO maser sources with velocity separations of 73 and 147 km s⁻¹. Judging from the large velocity separation of the peaks of these sources, we infer

that the two peaks probably do not originate in a single outflow, but are apparent doubles; two independent sources were seen by chance in a 40'' beam of the 45-m telescope. To confirm this, we performed radio mapping and near-infrared imaging observations. In this paper, we describe the radio and infrared observations of these interesting pair sources.

We also wish to point out the potential application of the VLBI technique for these stars, i.e., a possibility to measure the proper motions and parallaxes of stars with VLBI. Once two or more maser sources have been detected in one telescope beam of a single antenna, it is, in principle, possible to measure the relative position between the sources with VLBI with high accuracy. Pairs of sources are quite difficult to find at frequencies of 22 and 43 GHz, because of the small (~1') telescope beam size (though there is an exception of a SiO maser-source cluster at the galactic center; Menten et al. 1997; Izumiura

et al. 1998). These double sources may be used for future astrometric experiments.

2. Observations and Data Reductions

2.1. Radio Observations

The observations in the SiO $J=1-0$ $v=1$ and 2 transitions at 43.122 and 42.821 GHz were made with the Nobeyama 45-m radio telescope during the period of the SiO maser survey of the bulge and disk IRAS sources during 1992–1997 (see the detail of observations given by Izumiura et al. 1994, 1999). A cooled SIS receiver with a band width of about 0.4 GHz was used, and the system temperature was about 200–500 K, depending on the weather. The aperture efficiency of the telescope was about 0.60 at 43 GHz. The telescope half-power beam width was about $40''$. A factor, 2.9 Jy K^{-1} , was used to convert the antenna temperature to the flux density. An acousto-optical spectrometer array having high resolution (AOS-H) was used. Each spectrometer had a 40 MHz band width and 2048 frequency channels, giving an effective spectral resolution of about 0.3 km s^{-1} at 43 GHz. The telescope pointing was checked against the strong maser source VX Sgr, and was confirmed to have an accuracy of about $5''$.

The first detection of the double components of IRAS 18465–0717 at $V_{\text{lsr}} = 8$ and -65 km s^{-1} was made in 1992 May. The second observation was in 1993 April to check the time variation and the position. The relative intensities of the two peaks did not seem to have changed over a one-year period. Detection of the double components of IRAS 18019–1822 was made in 1997 May. The integrated spectra of both sources are shown in figure 1 and the line parameters are given in table 1; the higher and the lower velocity components are designated A and B, respectively, for each source.

A five-point mapping observation (separated by the half-beam size) was made in 1993 May for IRAS 18465–0717. The B component ($V_{\text{lsr}} = -65 \text{ km s}^{-1}$ component) was found to be located south east of the A component ($V_{\text{lsr}} = 8 \text{ km s}^{-1}$; see figure 2). A Gaussian fit of the intensities at each position gave the separation of the two sources as $20''$. The mapping results are summarized in table 2. The pointing accuracy of the 45-m telescope system depends strongly on the wind; we estimate that it was about $\sim 5''$. The spectra of the SiO $J=1-0$ $v=1$ transition exhibited a poor signal-to-noise ratio during the time of observation. Therefore, we used only the $J=1-0$ $v=2$ data for the analysis. Because of the weakness of the SiO intensities of 18019–1822, we did not attempt to map it. The IRAS positions and flux densities at 12, 25, and $60 \mu\text{m}$ for the two sources are summarized in table 3.

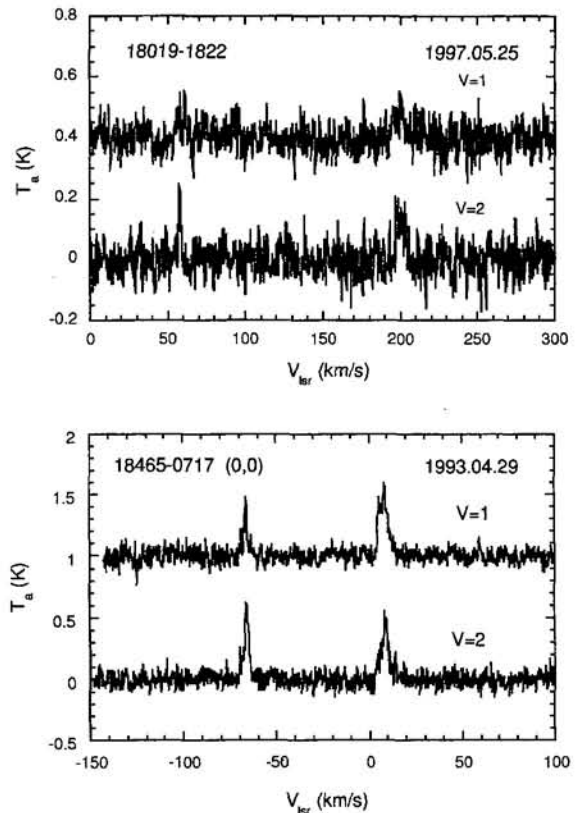


Fig. 1. Spectra of the SiO $J=1-0$ $v=1$ and 2 transitions in IRAS 18019–1822 (upper panel) and 18465–0717 (lower panel).

2.2. Near-Infrared Observations

Near-infrared photometric observations of IRAS 18019–1822 and 18465–0717 were made with the ANU (Australian National University) 2.3-m telescope at Siding Spring Observatory, Australia, on 1997 June 18–23. The infrared array camera, CASPIR (the Cryogenic Array Spectrometer/Imager), uses a 256×256 InSb detector array with $0''.5$ per pixel, covering a field of view of $128'' \times 128''$. The seeing size of a star image was about $1''-1''.5$. The limiting magnitudes for the J , H , and K bands were about 17, 16, and 14, respectively. The details concerning the observations and data reductions are described in Deguchi et al. (1998).

Identifications of the sources were made in terms of the K magnitude and the color, $H - K$, of the source, which were based on previous experiences of identifications of SiO maser stars on near-infrared images (Jiang et al. 1997; Deguchi et al. 1997). The accuracies of the positions of the IRAS sources given in the IRAS Point Source Catalogue are known to be about $10''$ (Beichman et al. 1988). The field of view of CASPIR ($128'' \times 128''$) is sufficient to locate the near-infrared counterpart near to the center of the field.

Table 1. Results (radio observations).

IRAS name	No	SiO $J = 1-0$ $v = 1$				SiO $J = 1-0$ $v = 2$			
		T_a	S	V_{lsr}	RMS	T_a	S	V_{lsr}	RMS
		(K)	(K km s $^{-1}$)	(km s $^{-1}$)	(K)	(K)	(K km s $^{-1}$)	(km s $^{-1}$)	(K)
18019–1822	A	0.169	0.71	200.4	0.035	0.207	0.77	196.9	0.042
	B	0.154	0.36	53.7	0.035	0.246	0.39	57.5	0.042
18465–0717	A	0.605	3.08	8.3	0.053	0.548	2.37	8.2	0.051
	B	0.485	1.01	–65.8	0.053	0.618	1.92	–65.9	0.051

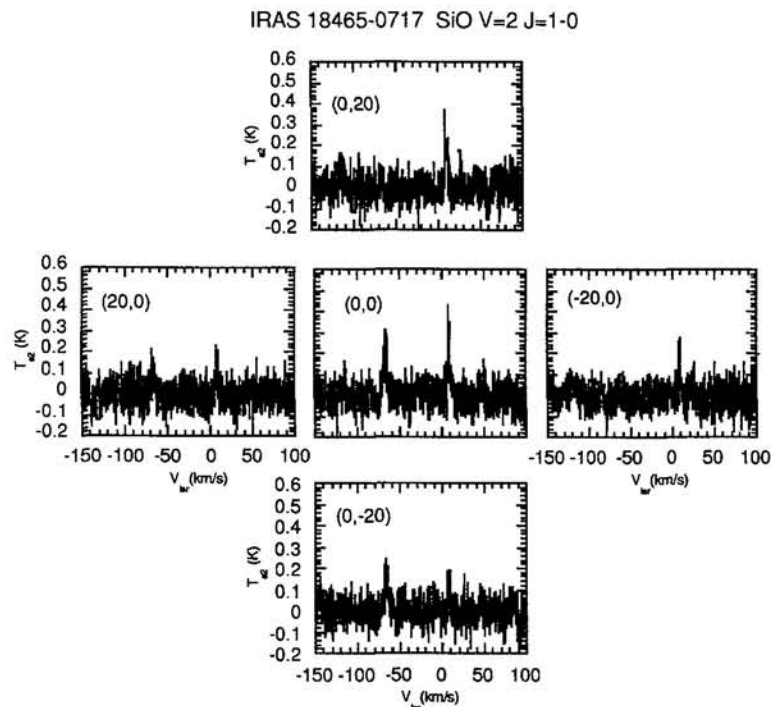


Fig. 2. The five point map of IRAS 18465–0717 in the SiO $J = 1-0$ $v = 2$ transition. The position differences from the IRAS position in unit of $''$ are indicated in parentheses. The source B (-65 km s $^{-1}$) is located $\sim 20''$ south east of the component A (8 km s $^{-1}$).

We found candidates for the near-infrared counterparts of 18019–1822 and 18465–0717. The results are summarized in table 4. The difference from the IRAS PSC position, ΔRA and ΔDec ($''$), the measured J , H , and K magnitudes, and the colors, $J - H$ and $H - K$, and the confidence level are listed. The center position of a candidate star was measured by fitting the Gaussian intensity profile on the star image. In order to determine the position error of the telescope pointing from the IRAS position, we compared the J -band image with the same field of the DSS (Digitised Sky Survey) image. Then, the offsets were determined from the positions of the optical reference stars in the DSS image. The proper motions of

the reference stars were neglected.

The confidence level, which is defined as unity minus the contamination probability of the field stars (for the definition, see Deguchi et al. 1998), was calculated, and is given in the last column of table 4. From the field star density in the galactic plane, we calculated the contamination rate, i.e., the probability of the field star being found within the distance between the IRAS PSC position and the candidate position. The details are described in Deguchi et al. (1998). The confidence level is, however, just an indicator of the star being associated with IRAS sources.

In both cases of IRAS 18019–1822 and 18465–0717,

Table 2. Mapping results for IRAS 18465 – 0717.

Source	V_{lsr}	ΔRA	ΔDec	Comment
	(km s^{-1})	($''$)	($''$)	
A	10	$-3.0 (\pm 3.1)$	$5.8 (\pm 0.1)$	
B	-65	$12.5 (\pm 8.1)$	$-10.9 (\pm 3.3)$	OH 1612 MHz by Le Squeren et al. (1992)
Difference.....		$15.5(\pm 8.7)$	$16.8(\pm 3.3)$	

Table 3. Infrared (IRAS) properties.

IRAS name	RA (1950)	Decl (1950)	l	b	F_{12}	F_{25}	F_{60}	LRS
	(h m s)	($^{\circ}$ ' ")	($^{\circ}$)	($^{\circ}$)	(Jy)	(Jy)	(Jy)	
18019–1822	18 15 07.9	-18 22 43	11.34	+1.52	5.1	5.7	4.8	
18465–0717	18 46 34.6	-7 17 18	26.25	-2.81	16.3	16.7	4.0	13

we found a very bright, red star near to the center of the image. It is almost certain that one of the double SiO maser peaks comes from this bright star; the confidence levels are above 99.5%. The photon counts were saturated for both sources in H and K [causing bluish color in figure 3 (Plate 12)] and the lower limits of the H and K magnitudes are given in table 4.

For IRAS 18465–0717, because the candidate for the second SiO maser peak is located very close (within $4''$) to the IRAS position, this is a highly probable candidate. Judging from the relative positions of the SiO peaks determined with the Nobeyama telescope, component A corresponds to candidate 1, and component B to candidate 2. Another faint red object is recognizable by $20''$ south-east of candidate 2 in the lower panel of figure 3 (Plate 12). Because of the large separation from the expected position and the faintness ($K \sim 12.50$ mag), the confidence level of this source as a candidate is low ($\leq 55\%$). Therefore, we exclude this star from the candidate list.

There are three candidates for the second SiO source associated with IRAS 18019–1822, as shown in table 4. Candidate 2 is about $30''$ west of the IRAS position. The color $H - K$ of 0.68 for this star is within the expected range for SiO maser sources, but it is possible that this is a normal star suffering interstellar reddening. Because the half-power beam width (HPBW) of the 45-m telescope is $40''$, there is only a small chance that this is the star responsible for the second SiO peak of IRAS 18019–1822. The other close-by candidates 3 and 4, are detected only on the K -band image. No stars were found at the same positions in the H -band image. The limiting magnitude of the H -band image was estimated to

be 16.8 mag, giving $H - K$ more than 4 mag for these stars. Further radio observations with better positional accuracy of the SiO sources are required to fix the candidates.

3. Discussion

The distances to these sources are difficult to estimate. The van der Veen and Breukers (1989) method, which utilizes IRAS 12 and 25 μm fluxes, gives the luminosity distances, 7.3 and 3.8 kpc for 18019–1822 and 18465–0717, respectively. Here, we assume that the luminosity of the source is $8 \times 10^3 L_{\odot}$. However, the IRAS flux is the sum of the two fluxes from double sources, so that their real distances may be much larger (by a factor of 1.4 when the contributions to infrared intensities from double sources are even).

3.1. Previous Observations at Other Wavelengths

The OH 1612 MHz maser has been detected in IRAS 18465–0717 at $V_{\text{lsr}} = -78.0$ and -54.8 km s^{-1} (Le Squeren et al. 1992). The center velocity, -66.4 km s^{-1} , coincides with the B component of SiO at -65 km s^{-1} . The spectra of OH 1612 MHz emission given by Le Squeren et al. (1992) exhibited a standing-wave feature at the high-velocity side of the spectrum, and it is difficult to judge whether or not any features exist at the higher velocity side of the above-mentioned OH double peaks. The beam of the telescope (Nançay) was by $4' \times 11'$ in this OH observation, enough to locate the A component in the same telescope beam.

The IRAS Low Resolution Spectrum (LRS) of 18465–0717 exhibits a flat featureless spectrum between

Table 4. Result (Infrared observations).

IRAS name	No	Δ RA (")	Δ Dec (")	J (mag)	H^* (mag)	K^* (mag)	$J - H$ (mag)	$H - K$ (mag)	Conf. Lev. (%)
18019–1822	1.....	0.9	–0.1	8.53	>6.81	>5.94	>1.72	>0.87	99.9
	2.....	–27.5	–12.5	11.65	9.77	9.09	1.87	0.68	83.6
	3.....	5.4	–17.5	—	—	2.81	—	>4.0	55.9
	4.....	20.5	5.7	—	—	12.02	—	>4.7	75.7
18465–0717	1.....	–2.1	13.1	8.67	>6.87	>6.20	>1.81	>0.66	99.7
	2.....	3.2	–1.1	—	12.21	9.68	—	2.53	99.8

*Inequality in H and K magnitudes indicates a saturation in detector counts.

8–23 μm , giving an LRS class of 13. The IRAS LRS spectrum must, however, be a composite of two spectra from different sources, making the classification difficult.

No literature on previous observations of IRAS 18019–1822 was found.

3.2. Comparison with the Bipolar Maser Sources

The velocity separations of the double peaks of normal OH/IR sources are usually about 10–50 km s^{-1} (e.g., Reid, Moran 1981). The OH/ H_2O spectra of some bipolar objects [IRAS 16342–3814, 18450–0148 (W43A), 19134+2131; Likkell et al. 1992], however, exhibit double peaks with separations of 100–260 km s^{-1} , originating from a high-velocity outflow. The large velocity separations (more than 100 km s^{-1}) seen in these bipolar objects are believed to occur only during the final stages of mass loss on the AGB or during the early post-AGB phases.

The velocity separations of about 70 and 150 km s^{-1} , which were observed in the two SiO maser sources in the present paper, are comparable with the velocity separations of these bipolar objects. This fact leads to the possibility that these doubly peaked SiO sources may not be apparent doubles, but bipolar objects with a high-velocity outflow. However, we dismiss this suggestion for the following reasons.

For the case of IRAS 18465–0717, we have shown that the two peaks of SiO come from positions separated by about 20", indicating that they are not of bipolar origin. In the case of IRAS 18019–1822, we cannot completely rule out the bipolar possibility, because no mapping observation has been made and the infrared counterpart for the second source was somewhat dubious. However, SiO maser emission is rare in bipolar objects with doubly peaked OH/ H_2O spectra (e.g., see Nyman et al. 1998), a fact that provides a strong case against the possibility of a bipolar origin. The observed lack of SiO emission from bipolar objects is consistent with the belief that the inner envelopes of stars at the transient (protoplanetary)

phase are partly ionized, and SiO maser action is therefore unexpected.

There are a few exceptions of so called protoplanetaries, such as OH 231.8+4.2 and OH 15.7+0.8, which exhibit SiO maser emission (Barvainis, Clemens 1984; Nyman et al. 1998). In fact, OH 231.8+4.2 is a known double star system, with a pulsating AGB star of late M spectral type as the SiO source, and a blue companion star creating the bipolar outflow (Cohen et al. 1985). The center velocity of the SiO masers from these sources is close to the mean velocity of the OH double peaks (close to the stellar velocity), and the width is about 10–20 km s^{-1} . On the other hand, the SiO double peaks in IRAS 18019–1822, with a separation of about 150 km s^{-1} , are quite different from the above-mentioned OH sources. The only way that a single bipolar object could give rise to such a high velocity separation would be if the SiO emission was emitted from the front and rear parts of a high-velocity flow; however, no bipolar object has ever been observed with such a large velocity separation in the SiO lines. Finally, we note that the IRAS colors of the bipolar objects, $[\log(F_{25}/F_{12}) \sim 0.3\text{--}1.1]$ are much redder than the colors of the doubly-peaked SiO sources (~ 0.0) discussed here.

Given the above reasoning, it seems to be most natural to interpret the doubly peaked SiO objects as being apparent doubles, and not bipolar objects.

3.3. Density of Apparent Doubles

The probability of detecting double SiO sources in a beam can be calculated from the source surface density. Suppose that the IRAS sources in a certain color range in the galactic disk are all late-type stars, and that half of these sources emit SiO maser radiation. The IRAS point sources with colors of $-0.3 < C_{12} < 0.2$ and $-0.1 < C_{23} < 1.0$ are potential candidates for SiO maser emitters (our experience showed 50% detection probability with the 45-m telescopes for these sources). The number count of IRAS sources with $F_{12} > 2$ Jy in the area of

$10^\circ < l < 30^\circ$ and $|b| < 3^\circ$ gives 2049 sources which satisfy the above criteria. The source surface number density is about 17 sources per square degree, or 0.014 per square arcminute. Assuming that half of the sources are SiO maser emitters, the probability of detecting double sources in a telescope beam of $1'$ (taken to be slightly larger than the real HPBW of the telescope, due to the Gaussian beam shape) is about 0.003 per source. We have currently observed approximately 300 IRAS sources in a sky strip of $-10^\circ < l < 30^\circ$, so that the expected number of cases for double detections is one. This is roughly consistent with the two cases of double detections discussed in the present paper.

Shiki et al. (1997) found 6 SiO maser sources toward the Sgr B2 molecular cloud. From this observation, the average surface density of SiO maser sources in the galactic disk at $l \sim 0.6$ was derived as 56 SiO sources per square degree, which is consistent with the surface number density of OH/IR sources, 45 per square degree, in the galactic nuclear disk (Lindqvist et al. 1992). The number densities of OH/IR or SiO sources in the nuclear disk, about 50 per square degree ($l \sim 0.6$), seem to be compatible with the surface number density, 17 sources per square degree of IRAS sources in the galactic disk ($l \sim 10^\circ\text{--}30^\circ$). When we take into account the SiO detection rate of about 50% in these IRAS sources, the SiO maser source density in the galactic plane for $l \sim 10^\circ\text{--}30^\circ$ is estimated to be about half of the SiO or OH/IR surface density at the edge of the nuclear disk.

3.4. Future Astrometry at Radio Wavelengths

A problem with the contemporary VLBI technique for astrometric applications is the correction of the atmospheric phase delay in the ionosphere. This effect can be calibrated for continuum-source measurements employing two well-separated frequencies. With this technique, the extragalactic reference frame has been well established (Johnston et al. 1995; Sovers et al. 1998). For compact, galactic line sources, such as OH/H₂O/SiO masers, however, the technique does not work, because they emit narrow lines. Until the present, the absolute positions of SiO maser sources have been known only to an accuracy of about $0''.1$ with normal mm-wave interferometers or the VLA (for example, see Wright et al. 1990; Baudry et al. 1995). The measured SiO maser positions are consistent with the Hipparcos star positions within the observational errors (Sutton 1997). The proper motions and parallaxes of maser stars have never been observed with VLBI (except with the phase-reference technique for special OH/IR sources; see van Langevelde et al. 1997; Sjouwerman et al. 1998).

Once two or more maser sources are detected in one telescope beam of a single antenna, it is, in principle, possible to measure the relative position between the sources

with VLBI with high accuracy. Pairs of sources may be relatively easily found among the OH masers at 1.6 GHz, where the telescope beam sizes are large (of about $3'\text{--}30'$). However, the spread of OH 1612 MHz maser emission on the scale of about 10^{16} cm makes any precise astrometric position measurement difficult. The H₂O and SiO masers at 22 and 43 GHz, respectively, are more useful for astrometric purposes, because the maser spots are spatially more confined ($\sim 10^{14}$ cm) than the OH spots; the central star is considered to be located at the center of the maser spot ring (Diamond et al. 1994). Double H₂O or SiO maser sources in a single beam are, however, very rare because of the smaller telescope beam size due to higher frequencies. In one unique case, 7 SiO masers in a single beam of the 45-m telescope are found at the galactic center (Izumiura et al. 1998); these sources have been used to connect in the galactic center the radio and optical reference frames to an accuracy of better than $0''.1$ with the VLA (Menten et al. 1997). However, we cannot generally expect such late-type star clusters in the galactic disk.

The apparent-double SiO maser sources are probably important for astrometric use. They provide the possibility to measure relative positions with an accuracy of about $100 \mu\text{as}$ with the present-day VLBI. We should, however, note that the parallaxes and proper motions can be measured with VLBI only relative to the more distant source of the SiO pair; the distance from the Sun to the closer source can be obtained from the parallax if the other source is quite distant (virtually infinite; otherwise the upper limit of the distance). Though the flux densities of the SiO masers found in this paper are low, about a few Jy for IRAS 18465–0717, the widths of the lines are relatively large (more than 10 km s^{-1}). A VLBI experiment involving a phased Very Large Array could detect these SiO maser emissions and measure the relative distances between the two sources.

The parallax and proper motions will be measurable in the future. The presently planned VLBI project, VERA (VLBI Exploration of Radio Astrometry; see Hara et al. 1988), aims to rectify the random phase delay due to the ionosphere by fast position switching between SiO maser sources and reference continuum sources, enabling measurements of the absolute positions of maser sources with an accuracy of $10 \mu\text{as}$. The sensitivity of VERA will probably be down to 3 Jy with four 20-m antennas (Miyoshi 1998, a poster paper at JAS meeting). The double SiO sources found here are still a little weak for VERA observations, but should be useful for future studies with VERA combined with larger aperture antennas, such as the Kashima 34-m and NRO 45-m telescopes.

4. Conclusion

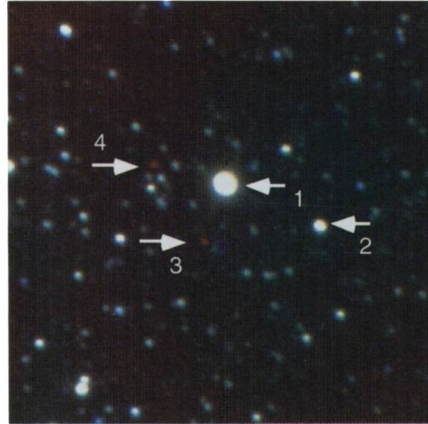
We have found two cases of doubly peaked SiO maser emission toward single IRAS point sources; in each case, the detections were made in a single telescope beam of $\text{HPBW} = 40''$. The two emission components have a velocity separation of 70–150 km s^{-1} . Because these sources are near to the galactic plane, where IRAS sources are relatively crowded, they correspond to pairs of stars, each with an SiO maser source. Infrared imaging observations were used to locate the candidates for each source. These SiO maser sources should be useful in future for high-precision astrometry with VLBI at 43 GHz.

The authors thank the maintenance staff for their kind assistance during the observations at MSSSO. They also thank T. Tanabe, M. Miyoshi, and O. Kameya for discussions and encouragements. This research was supported by a Grant in-aid for Scientific Research (C) (No. 10640238) of the Ministry of Education, Science, Sports and Culture. One of authors (SD) received international travel grants from the Monbusho International Scientific Research Program (P.I.: K. Kodaira). This research was made use of SIMBAD database, operated at CDS, Strasbourg, France.

References

- Barvainis R., Clemens D.P. 1984, *AJ* 89, 1833
 Baudry A., Mazurier J.M., Perié J.P., Requième Y., Rousseau J.M. 1990, *A&A* 232, 258
 Beichman C.A., Neugebauer G., Habing H.J., Clegg P.E., Chester T.J. 1988, *IRAS Catalogs and Atlases, I. Explanatory Supplement*, NASA RP-1190 (US Government Printing Office, Washington) pVII-22
 Cohen M., Dopita M.A., Schwartz R.D., Tielens A.G.G.M. 1985, *ApJ* 297, 702
 Deguchi S., Matsumoto S., Wood P.R. 1998, *PASJ* 50, 597
 Deguchi S., Shiki S., Matsumoto S., Jiang B.W., Nakada Y., Wood P.R. 1997, *PASJ* 49, 561
 Diamond P.J., Kembell A.J., Junor W., Zensus A., Benson J., Dhawan V. 1994, *ApJ* 430, L61
 Elitzur M., Goldreich P., Scoville N. 1976, *ApJ* 205, 384
 Hara T., Okamoto I., Sasao T. 1988, *Vistas Astron.* 31, 647
 Izumiura H., Deguchi S., Fujii T. 1998, *ApJ* 494, L89
 Izumiura H., Deguchi S., Kameya O., Matsumoto S., Nakada Y., Ootsubo T., Ukita N. 1999, *ApJ* submitted
 Izumiura H., Deguchi S., Hashimoto O., Nakada Y., Onaka T., Ono T., Ukita N., Yamamura I. 1994, *ApJ* 437, 419
 Jiang B.W., Deguchi S., Hu J.Y., Yamashita T., Nishihara E., Matsumoto S., Nakada Y. 1997, *AJ* 113, 1315
 Johnston K.J., Fey A.L., Zacharias N., Russell J.L., Ma C., De Vegt C., Reynolds J.E., Jauncey D.L. et al. 1995, *AJ* 110, 880
 Le Squeren A.M., Sivagnanam P., Dennefeld M., David P. 1992, *A&A* 254, 133
 Likkell L., Morris M., Maddalena R.J. 1992, *A&A* 256, 581
 Lindqvist M., Habing H.J., Winnberg A. 1992, *A&A* 259, 118
 Menten K.M., Reid M.J., Eckart A., Genzel R. 1997, *ApJ* 475, L111
 Nyman L.-Å., Hall P.J., Olofsson H. 1998, *A&AS*, 127, 185
 Reid M., Moran J.M. 1981, *ARA&A* 19, 231
 Shiki S., Ohishi M., Deguchi S. 1997, *ApJ* 478, 206
 Sjouwerman L.O., van Langevelde H.J., Diamond P.J. 1998, *A&A* 339, 897
 Sovers O.J., Fanselow J.L., Jacobs C.S. 1998, *Rev. Mod. Phys.* 70, 1393
 Sutton E.C. 1997, *PASP* 109, 1085
 van der Veen W.E.C.J., Breukers R.J.L.H. 1989, *A&A* 213, 133
 van Langevelde H.J., Brauher J., Diamond P.J., Schilizzi R.T. 1997, in *IAU Symp.* 180, ed H.J. Habing, H.J.G.L.M. Lamers (Kluwer, Dordrecht) p373
 Wright M.C.H., Plambeck R.L., Mundy L.G., Looney L.W. 1995, *ApJ* 455, L185

18019-1822



18465-0717



Fig. 3. The Near Infrared images ($128'' \times 128''$) for IRAS 18019–1822 (upper panel) and 18465–0717 (lower panel). The *J*, *H*, and *K* images are synthesized into a false RGB color image. The color tone is adjusted in each image so that the relative color difference between different images is arbitrary. North is up and the east is left.

S. DEGUCHI et al. (See Vol. 51, 358)